

Assessment of the relative contribution of cellular components to the acetowhitening effect in cell cultures and suspensions using elastic light-scattering spectroscopy

Tao T. Wu and Jianan Y. Qu*

Department of Electronic and Computer Engineering, Hong Kong University of Science and Technology, Clear Water Bay, Kowloon, Hong Kong, China

*Corresponding author: eequ@ust.hk

Received 6 October 2006; revised 15 February 2007; accepted 8 March 2007;
posted 16 March 2007 (Doc. ID 75826); published 6 July 2007

We aim to investigate the mechanism of acetowhitening upon which the colposcopic diagnosis of cervical cancer is based. The changes in light scattering induced by acetic acid in intact cervical cancer cells and cellular components were studied using elastic light-scattering spectroscopy. After adding acetic acid to intact cancer cell culture samples (cell suspensions and attached monolayer cell cultures), a slight decrease in small-angle forward scattering was observed, while the large-angle scattering increased by a factor of 5–9, indicating that acetowhitening signals are mainly contributed from small-sized intracellular scattering structures. The cellular components of different sizes and masses were isolated to investigate their individual contribution to the changes of light scattering induced by acetic acid. The study provided the evidence that the cellular components of diameter smaller than 0.2 μm in the cytoplasm are the major contributors to the acetowhitening effect in whole cells, while the light scattering from the mitochondria are not sensitive to the acetic acid. © 2007 Optical Society of America

OCIS codes: 290.1350, 120.5820, 160.4760, 170.4580.

1. Introduction

Acetic acid is a key diagnostic reagent used in colposcopy to induce the acetowhitening effect and to enhance the contrast between early cervical lesions and normal cervix tissue. The acetowhitening phenomenon, where the abnormal tissue usually turns white while the normal tissue remains almost unchanged, is transient and reversible [1]. There are two possible mechanisms for the acetowhitening effect at the cellular level [2]: (1) the acetowhitening is mainly caused by cytokeratins in the cytoplasm of epithelial cells due to their filamentous architecture. A slight decrease in the pH increases the polymerization, through which the cytokeratins form a network of cytoplasmic filaments in the cell. The thickness and optical properties of the filaments change with the degree of polymerization; (2)

in the nuclei, a slight decrease in the pH provokes deacetylation of the histones, which results in a dense chromatin structure and changes their optical properties [3]. These changes disappear when the acetic acid is completely neutralized, therefore making the effect temporary [2].

It was recently found that the dynamic change in the backscattering light intensity induced by acetic acid could be quantified for guiding colposcopic diagnosis to distinguish between abnormal and normal cervical tissue in clinical settings [4,5]. We have also investigated the dynamic changes of total backscattering intensity in both normal- and cancerous-cultured monolayer cells [6]. These studies suggest that quantitative measurement of the acetowhitening process can help us make the colposcopic procedure objective and improve this diagnostic technique's performance. Because a fundamental understanding of the mechanism of the acetic-acid-induced changes of light scattering from cells is essential, in this work, we investigate what

component in the cervical squamous cell carcinoma line (SiHa) contributes to the acetowhitening and how sensitive the changes of cells' optical properties are to acetic acid. The method we used here is elastic light-scattering spectroscopy (LSS).

The noninvasive LSS technique is an important tool for studying the optical scattering from cellular organelles. It has been used to investigate cellular structures in a variety of tissues or cultured cells [7–15]. In this work, we focus on the acetic-acid-induced changes in light scattering from intact cells and their isolated organelles. In particular, we address the issue of which component in the cells is the major contributor to the acetowhitening effect. We measure the wavelength-dependent light-scattering signals from the attached monolayer cells in culture medium and intact cells and their isolated organelles suspended in phosphate-buffered saline (PBS) solution from forward- to backward-scattering angles. Finally we obtain correlations between the changes of the scattering signal induced by acetic acid and the cell component fractions. Our analysis will indicate which cellular organelles are the major contributors to acetic-acid-induced whitening of cervical cancer cells.

2. Materials and Methods

A. Cell Culture Samples

A human cervical squamous cell carcinoma line (SiHa) was used in the experiments in this study. The SiHa cell line was obtained from the American Type Cell Collection [ATCC, USA], and the cells were maintained in Dulbecco's Modified Eagle's Medium [DMEM, Invitrogen Hong Kong Ltd., China] with supplements of 10% fetal bovine serum (FBS) at 37 °C in an atmosphere of 5% CO₂. Two types of cell samples were examined using light-scattering spectroscopy. The first type of cell sample was the attached monolayer cells cultured on an 18 mm × 18 mm coverslip of a microscope slide. The cells were cultured at different confluences. The second type was the intact cell suspensions in PBS. The cells were cultured to 80% confluence in 100 mm tissue culture dishes and then detached by incubation in a

prewarmed 0.25% trypsin solution containing 1 mM ethylenediamine tetra-acetic acid · 4Na for 5 min. After the addition of the complete medium, the cell suspensions were centrifuged (500 g for 5 min) and then washed twice by PBS and resuspended in PBS on ice until the light-scattering experiments.

B. Isolation of Cell Organelles

To investigate the detailed scattering characteristics of different cellular organelles, we performed LSS measurements on the isolated nuclear fraction and crude mitochondrial fraction (including lysosomes, peroxisomes, and other possible dense organelles, such as the Golgi apparatus and the rough endoplasmic reticulum with ribosomes bound to it). The cytoplasm except for the mitochondrial fraction (we call this the cytoplasmic fraction in this paper) was measured by LSS as well. The nuclear, mitochondrial, and cytoplasmic fractions were isolated from intact cells using a hypotonic medium and differential centrifugation [14,15].

Both phase contrast and fluorescence images were used to access the shapes and sizes of the organelles in the nuclear and mitochondrial fractions. Fluorescence images of intact cells and isolated nuclei were obtained using an inverted fluorescence microscope (eclipse TE2000-U, Nikon Instech Company, Ltd., Japan) at 60× and 100× magnifications. Hoechst 33342 dye (Invitrogen) was used to stain the nuclei. We captured the phase contrast images at the same time for comparison and verification. The mitochondria were stained with Rhodamine 123 (Invitrogen) and the fluorescence image was observed using a 100× objective lens that provided a resolution of ~0.2 μm. The fluorescence images are also used to verify the purification of the organelle isolation. There was no contamination by nuclear fragments in the mitochondrial and cytoplasmic fractions and vice versa.

C. Wavelength-Dependent Light-Scattering Measurements

A system schematic for LSS measurement is shown in Fig. 1. A 200 μm fiber conducted the broadband white light from a 75 W xenon arc source (model 60100, Oriel Instruments, USA) to an illumination

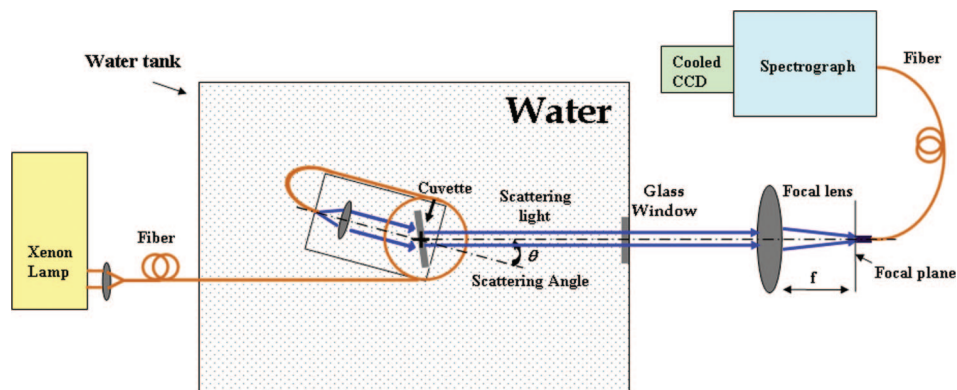


Fig. 1. (Color online) Schematic of the light-scattering spectroscopy setup.

unit. The light from the end of the fiber was then collimated by a 100 mm focal length lens and a series of apertures. The collimated light with a diameter of ~ 6 mm and a divergent angle of $\sim 0.06^\circ$ passed through a homemade cuvette (18 mm \times 15 mm \times 1.1 mm, width \times height \times thickness) containing the samples (attached monolayer cells or the cells and organelle suspensions). Both the collimator and the cuvette were fixed on a rotation stage. They were immersed in water to reduce the reflection from the surfaces of the cuvette and to minimize the displacement of optical paths of scattering light caused by the sample and cuvette when rotating the stage. The scattered light at a given angle was collected by a lens of 200 mm focal length and conducted by a 200 μm fiber to a spectrograph (model 77480, Oriel Instruments, USA) coupled with a cooled CCD camera (model NTE/CCD-1340/400-EMB, Roper Scientific, Inc., USA). The acceptance angle of the scattering collection unit was 0.06° , the same as the illumination unit. The scattering angle could be set by rotating the stage that the collimator and cuvette were fixed on. The exact scattering angle θ was determined by a micrometer of the rotation stage with an angular resolution of 0.02° . The system could measure the scattering light from the sample in the range of 1.1° and 165.0° .

The spectral measurement was calibrated by a Mercury Argon Calibration Source (HG-1, Ocean Optics Inc., USA). The spectral resolution of the spectrograph system was ~ 7 nm. The background signal taken from the cuvette with a pure culture medium or PBS solution was subtracted from the LSS signal measured from each sample. The system response was calibrated by normalizing the background-corrected LSS signal to the transmission spectrum measured at 0° with a pure culture medium (for attached monolayer cell cultures) or PBS solution (for cells and organelles suspension) in the cuvette. In the measurements, the glass cuvette was tilted to 25° to avoid the reflection of the illumination light from both surfaces of the cuvette and the reflection of strong forward scattering from the second surface of the cuvette. This arrangement effectively removed the interference of reflection from the measurement of backscattering signals.

The intensity and spectral line shape of light scattered from the large scattering centers varied drastically in the small forward-scattering angle. In this study, the forward scattering was measured in the angle range from 1.1° to 5.5° at an angular interval of $\sim 0.22^\circ$. The scattering spectra became featureless in the region of large-angle scattering from 6° to 165° . The angular interval was then set from 2° to 30° for the measurement of spectral signals in large-scattering angles. The measured scattering spectra were in the wavelength range from 400 to 700 nm. The integration time of the cool CCD was set from 0.01 s for a small-angle forward-scattering measurement to 30 s for a large-angle backscattering measurement. The absolute values of measured signal intensity were calibrated based on the response of the CCD at different exposure times.

LSS measurements were performed on the attached monolayer cell cultures, the suspensions of intact cells, and the suspensions of isolated fractions before and after the application of acetic acid, respectively. The concentrations of intact cells and isolated fractions in suspensions were determined to meet the condition that the illumination light only encountered single scattering when it passed through the suspensions. The method reported in [12–15] was used to determine the concentrations of intact cells and isolated nuclei in suspensions. We compared the light-scattering spectra from different concentrations of intact cells and isolated nuclei in suspensions. The maximal concentration was chosen such that a further dilution of the cells or isolated nuclei did not change the wavelength-dependent light-scattering spectral patterns at the forward- and backscattering angles [12–15]. It was found that the maximal concentration to avoid multiple scattering was 2×10^5 cells(nuclei)/ml, which were consistent with the reports from Mourant *et al.* [12,15], Drezek *et al.* [13], and Wilson *et al.* [14]. Here, the absolute concentration of cells or nuclei was manually measured using a standard hemocytometer and microscope. In the measurements of small-angle forward scattering, the cells and/or nuclei were further diluted to 0.5×10^5 to avoid the saturation of detector, and the concentration of 2×10^5 cells(nuclei)/ml was used in the measurements of large-angle scattering to ensure a high signal-to-noise ratio.

Because the sizes of the scatterers in mitochondrial and cytoplasmic fractions were small, no distinct oscillation patterns were observed in the scattering spectra that were monotonically decreasing the function of wavelength. We used the method described in [16] to determine the maximal concentration to meet the condition of single scattering in the cuvette loaded with mitochondrial or cytoplasmic fraction suspension. Specifically, mitochondrial and cytoplasmic fractions were diluted to make sure that the transmitted light intensity measured from the cuvette filled with samples was greater than 0.95 of the light intensity when the illumination light passes through the cuvette with pure PBS. The exact concentrations of mitochondrial and cytoplasmic fractions were unknown because the small-sized scatterers could not be clearly resolved by the microscope.

In previous work, we found that the acetowhitening signal reached the maximal level when acetic acid concentrations were 0.6% in the culture medium and 0.3% in the PBS solution [6]. The acetowhitening effect became completely irreversible, and permanent damage of cells was observed when acetic acid concentration was over 1.2%, a factor of 2–4 lower than the concentration clinically used in cervical tissue [6]. To ensure the acetowhitening signals reach a maximal level and to avoid cell damage, the concentration of acetic acid solution used in this study was set to 0.6% in the culture medium for the monolayer cells and 0.3% in PBS for the suspensions employing the same method reported in our previous work, respec-

tively. We found that the scattering spectra of cell and cellular fraction samples did not change over the course of LSS measurements (~25 min). This indicates that acetic acid may not cause cell damage at such low concentration levels used in our experiments.

3. Results and Discussion

A. Scattering from Cell Suspensions and Attached Monolayer Cell Cultures

In this study, wavelength- and angular-dependent light-scattering spectra from cell suspensions and attached monolayer cell cultures were measured using the LSS setup shown in Fig. 1. The representative light-scattering spectra from the intact cell suspension before and after the application of acetic acid are shown in Fig. 2. The intensity of angular-dependent scattering signals before and after the application of acetic acid are shown in Fig. 2(a). Here, the signal intensity at each scattering angle is an averaged intensity of light scattering over the wavelength range from 400 to 700 nm. As can be seen, acetic acid induced a significant increase of light scattering in large angles.

The detailed scattering spectra measured at representative scattering angles are displayed in Figs. 2(b)–2(h). Oscillation patterns were observed from small-angle forward scattering as shown in Figs. 2(b)–2(d). With the increase of the scattering angle from 1.1° to 4.4° , the oscillation pattern of forward scattering changed continuously. The scattering intensity decreased drastically (over almost 3 orders) in the range of the scattering angle from 1.1° to 12.0° . These indicate that forward scattering was dominated by large Mie-scattering particles such as whole cells and nuclei [13,17]. The signal intensity decreased slightly after the application of acetic acid, while the oscillation pattern in the scattering spectra remained almost unchanged. When the scattering angle was greater than 4.4° , the oscillation pattern disappeared, and the scattering spectra became a monotonically decreasing function of wavelength as shown in Figs. 2(e)–2(h). In particular, the intensity of large-angle scattering increased by a factor of 5–7 after the application of acetic acid. This indicates that small-sized scattering structures may be the major contributors to the changes of cell scattering induced by acetic acid because the scattering from small-sized scatterers are more angularly isotropic and decay monotonically in wavelength domain [11,16]. Though scattering of the cell and nucleus may dominate the signals in the small angles, it is overwhelmed by the scattering of small-sized scatterers in large angles.

In the study of scattering from attached monolayer cell cultures, LSS measurements were conducted in the same procedure as the measurements of scattering from cell suspension. We took LSS measurements from monolayer cell samples cultured at different confluences (from 70% to 100%) before and after the application of acetic acid. It was found that the confluence only affects the intensity of scattering signals, but did

not significantly affect the angular intensity distribution and the line shape of scattering spectra. The representative light-scattering spectra measured from a sample culture at 100% confluence are shown in Fig. 3. As can be seen, the results are similar to the scattering from cell suspension shown in Fig. 2. The angular distribution of light-scattering intensity displayed in Fig. 3(a) clearly demonstrates that acetic acid induces a significant increase of scattering in large angles, while the small-angle forward-scattering intensity decreased slightly after the application of acetic acid as shown in Figs. 3(b)–3(d). The oscillation pattern in small-angle forward scattering may be mainly contributed from the light scattering of nuclei because when the cells are cultured at 100% confluence, the boundary between cells becomes unclear, and the light scattering from the cell peripheral may be contributed to the total scattering signal as the scattering from small-sized structures. The oscillation pattern disappeared when the scattering angle was greater than 3.0° . The intensity of large-angle scattering increased approximately six to nine times after the application of acetic acid. This is consistent with the measurement results from intact cell suspensions.

B. Scattering from Suspensions of Cellular Fractions

Although LSS measurements of intact cells before and after the application of acetic acid revealed a significant increase of large-angle scattering induced by acetic acid, the origins remained unclear. In this study, we isolated the cellular components and investigated their individual contribution to acetic acid-induced changes of light scattering in cells. As described in Section 2, the cells were lysed with a hypotonic lysis buffer. The isolated nuclear, mitochondrial, and cytoplasmic fractions were obtained by using differential centrifugation and then diluted for the LSS measurements.

The light-scattering spectra of the isolated nuclear fraction before and after the application of acetic acid are shown in Fig. 4. The oscillation patterns were observed in the scattering spectra in small angles, which were similar to the light scattering of the intact cell samples. The acetic acid induced a slight decrease of light scattering in small angles and approximately a 2–3 factor increase in large-angle scattering. Representative scattering spectra of the isolated nuclear fraction are displayed in Figs. 4(b)–4(h).

The scattering spectral signals present no oscillation pattern in all scattering angles. The spectra remain in monotonic decay over the wavelength range from 400 to 700 nm. The angular-dependent scattering signals of the mitochondrial and cytoplasmic fractions before and after the application of acetic acid are shown in Fig. 5. In the mitochondrial fraction, the intensity of scattering signal only increased by approximately a factor of 1.3 after adding the acetic acid, while the scattering of cytoplasmic fraction increased by approximately a 6–8 factor in large-scattering angles. This indicates that scatterers in cytoplasmic fraction are more sensitive to the decrease of pH value after the application of acetic acid.

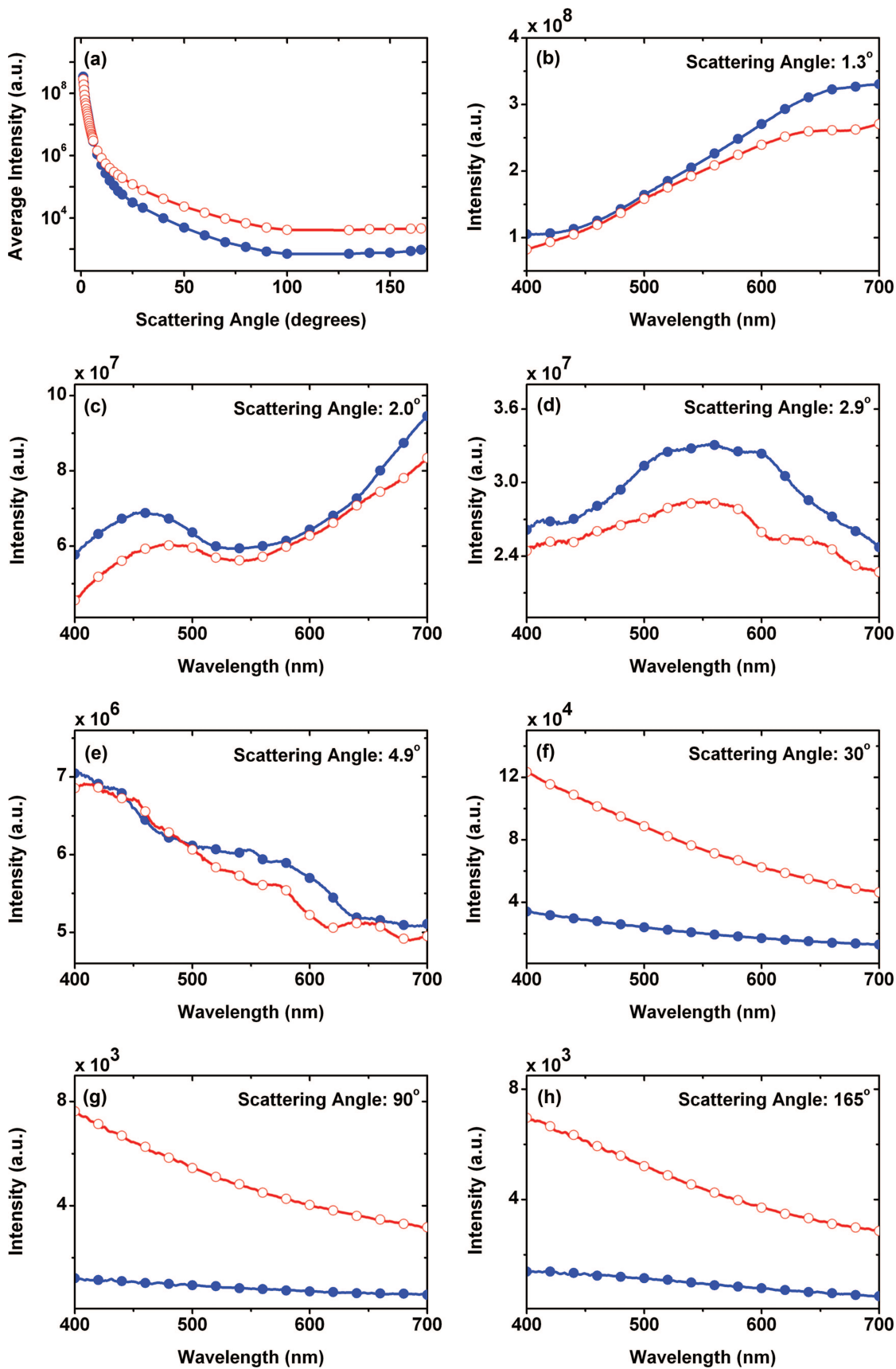


Fig. 2. (Color online) Light scattering from cell suspensions: (a) Angular-dependent light-scattering signals; (b)–(h) light-scattering spectra at multiple-scattering angles. Curves with solid circles: experimental data before the application of acetic acid. Curves with open circles: experimental data after the application of acetic acid.

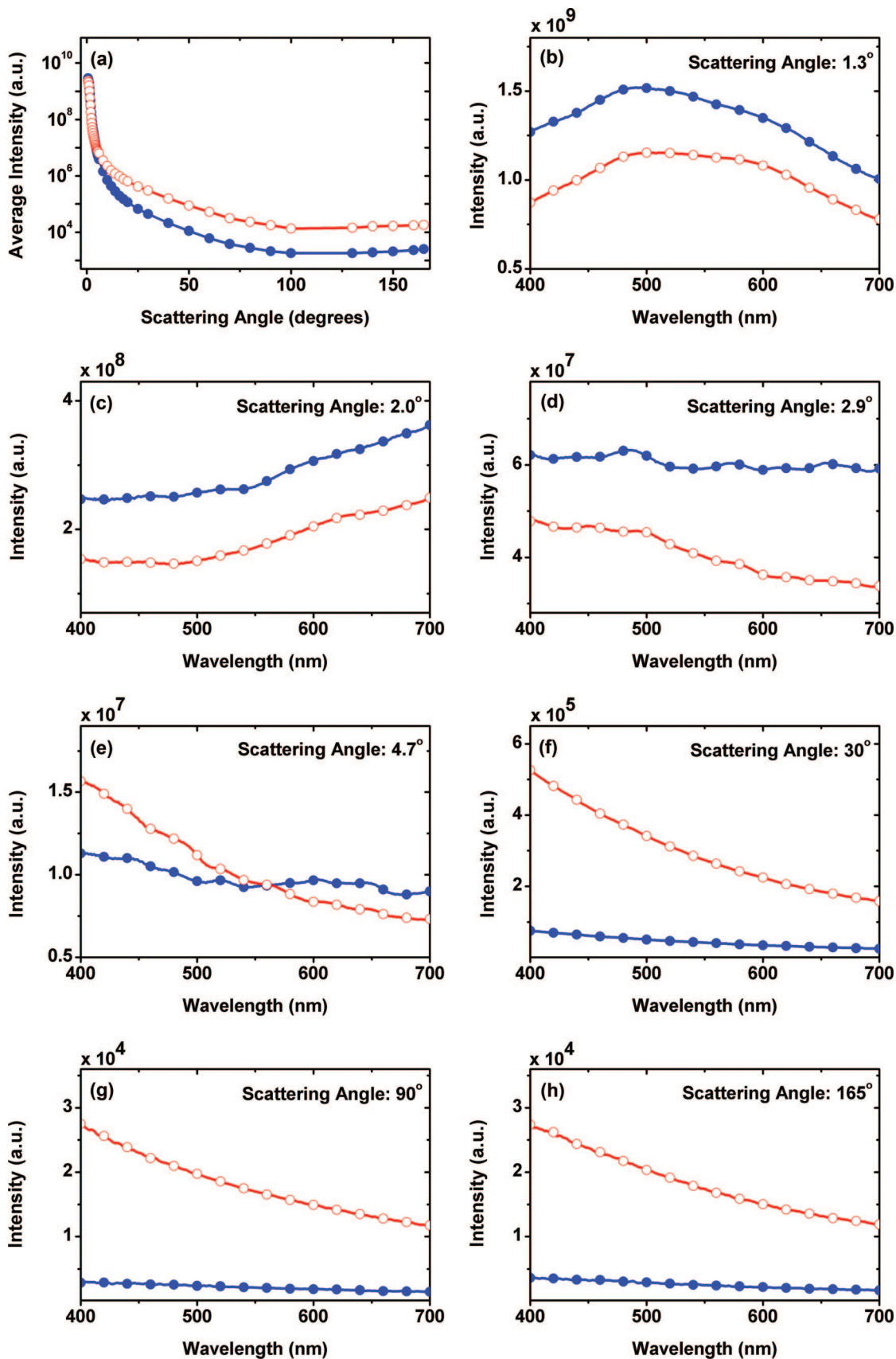


Fig. 3. (Color online) Light scattering from attached monolayer cells: (a) Angular-dependent light-scattering signals; (b)–(h) light-scattering spectra at multiple-scattering angles. Curves with solid circles: experimental data before the application of acetic acid. Curves with open circles: experimental data after the application of acetic acid.

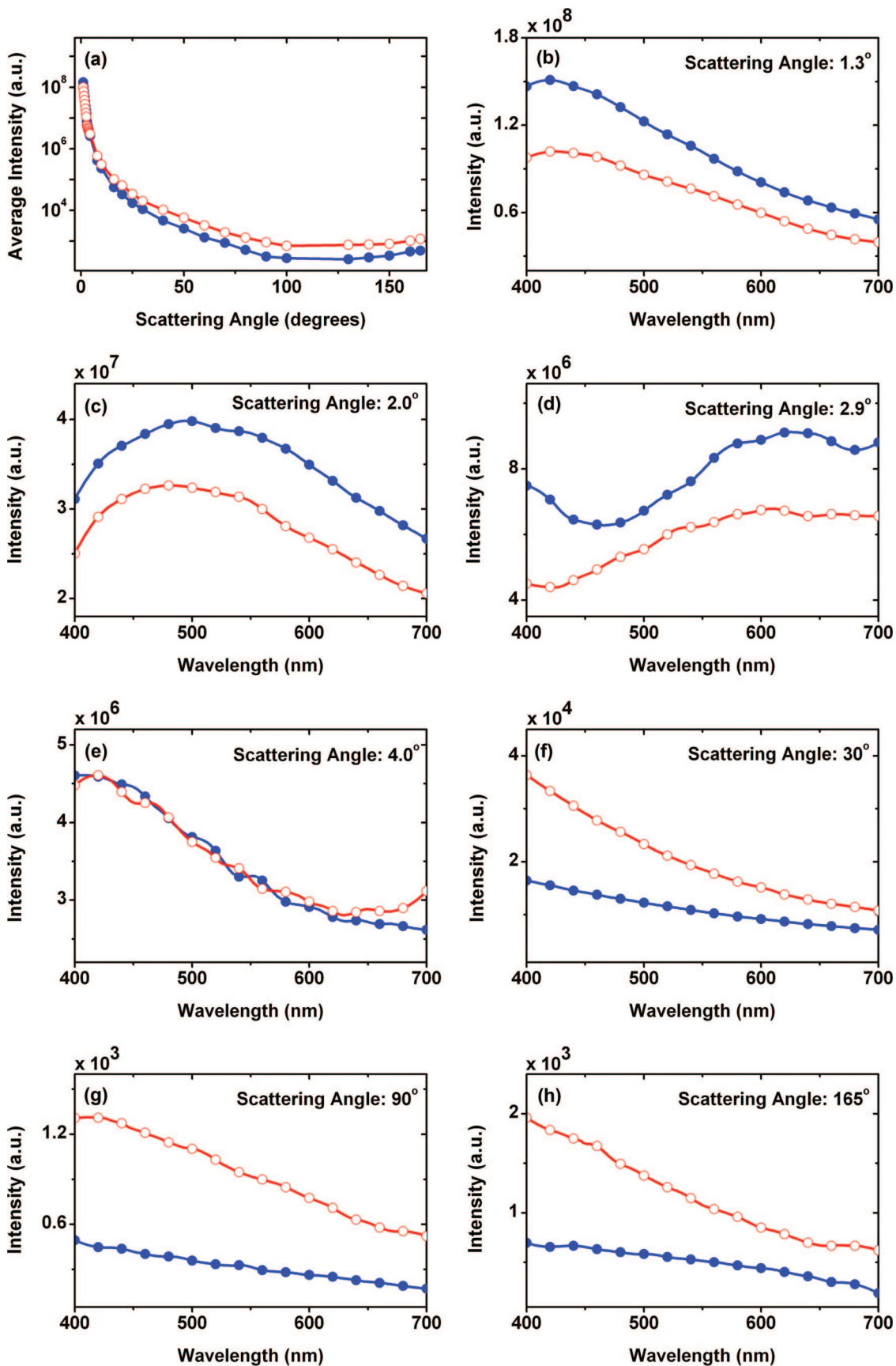


Fig. 4. (Color online) Light scattering from isolated nuclei suspensions: (a) Angular-dependent light-scattering signals (averaged intensity from 400 to 700 nm); (b)–(h) light-scattering spectra at multiple-scattering angles. Curves with solid circles: experimental data before the application of acetic acid. Curves with open circles: experimental data after the application of acetic acid.

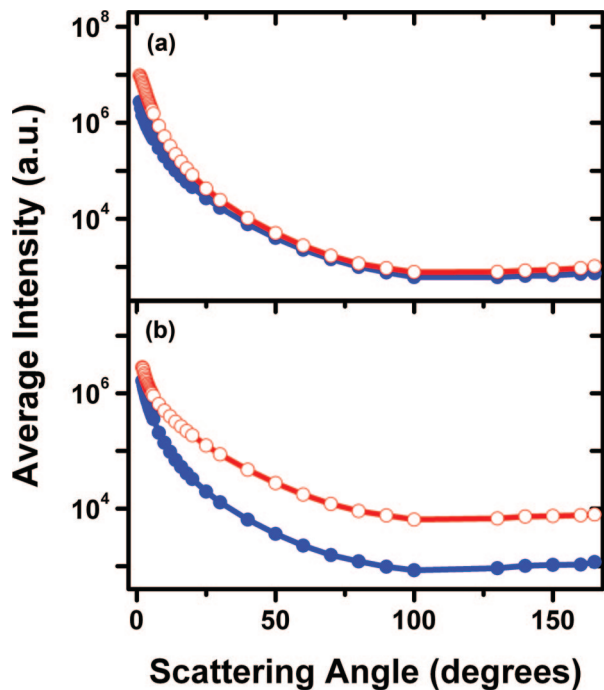


Fig. 5. (Color online) Angular-dependent light-scattering signals (average intensity from 400 to 700 nm): (a) mitochondrial fraction and (b) cytoplasmic fraction. Curves with solid circles: experimental data before the application of acetic acid. Curves with open circles: experimental data after the application of acetic acid.

C. Comparison of Large-Angle Scatterings

The results of LSS measurements show that the large-angle scattering spectra of intact cells, nuclear, mitochondrial, and cytoplasmic fractions do not present an oscillation pattern, indicating the small-sized scatterers are major contributors. The acetowhitening in precancerous cervical tissue is based on the increased backscattering of cancer cells induced by acetic acid. In this study, we calculated the intensity of the backscattering signal by integrating the angular-dependent scattering signals from 90° to 165° , the maximal scattering angle. The scattering signal intensity in the angle range is almost at the same level.

It was found that the relative ratio of backscattering intensity (nuclei:mitochondria:cytoplasm) was $\sim 1.0:1.9:2.9$ before adding acetic acid. Here, the scattering intensity of each cellular fraction was calculated by multiplying the ratio of its concentration after the procedure of cellular component isolation to the diluted concentration for LSS measurement. After adding acetic acid, the ratio changed to $2.5:2.5:20.9$ by taking the backscattering intensity of nuclear fractions before being exposed to acetic acid as a reference. Therefore, the increases of backscattering intensity induced by acetic acid are approximately 2.5, 1.3, and 7.2 times from nuclei, mitochondria, and cytoplasm, respectively. The LSS measurements of cell suspension and attached monolayer cell cultures showed that the backscattering increased by approximately a factor of 5.6 and 8.2 after the application of acetic acid, respectively. The acetic-acid-induced

increase of backscattering from the cytoplasmic fraction is similar to the increase from intact cells, demonstrating that the cytoplasmic fraction may be the major contributor to the acetowhitening effect in backward scattering of whole cells.

It should be noted that the refractive index of the solvent (PBS) in the isolated cellular fractions is different from those of cytoplasm and nucleoplasm. The actual contributions of the scatterers to the acetowhitening estimated from the study of isolated cellular fractions may not be completely the same as those in cells or cervical tissue. Finally, it should be emphasized that the acetowhitening characteristics measured in cell cultures and suspensions are different from the ones measured *in vivo*. Transport of acetic acid in tissue is largely determined by epithelial structures. Therefore, the acetowhitening in tissue is not only dependent on the increased cell scattering induced by acetic acid, but also dependent on the tissue morphology. A simple extrapolation of the findings in this study to the acetowhitening effect in living cervical epithelium could be misleading.

4. Conclusion

The scattering spectra measured from the cell suspensions and attached monolayer cell cultures show that the acetic acid induced a slight decrease of light scattering in small forward-scattering angles. The origin is unknown. The scattering of cells in the large angles increases significantly after the application of acetic acid. The scattering spectra measured from the cell suspension, attached monolayer cells, and the suspension of isolated nuclei show that Mie scatterings of cells and nuclei are dominant in the small forward-scattering angle ($<4.0^\circ$). The contributions from scattering of small-sized structures in cytoplasm become significant with the increase of scattering angle. The small-angle forward-scattering signals from cytoplasmic fraction are weak compared with those of nuclear and mitochondrial fractions because the sizes of scatterers in cytoplasmic fraction are small. Before the application of acetic acid, the backscattering of the cytoplasmic fraction is 2.9 and 1.5 times stronger than those of nuclear and mitochondrial fractions, respectively. After the application of acetic acid, the contribution to backscattering from cytoplasmic fraction is 8.3 times more than nuclear and mitochondrial fractions, respectively. It was found that mitochondria are not sensitive to the acetic acid and do not contribute significantly to the acetowhitening effect. The results provide evidence that small-sized cellular components in cytoplasm are the major contributors to the acetowhitening effect. The contribution from nuclear fraction is overwhelmed by cytoplasmic fraction.

The authors acknowledge support from the Hong Kong Research Grants Council through grants HKUST6052/02M and HKUST6408/05M.

References

1. M. C. Anderson, J. A. Jordan, A. R. Morse, and F. Sharp, *A Text and Atlas of Integrated Colposcopy: for Colposcopists*,

Histopathologists and Cytologists (Chapman & Hall Medical, 1992).

2. R. Lambert, J. F. Rey, and R. Sankaranarayanan, "Magnification and chromoscopy with the acetic acid test," *Endoscopy* **35**, 437–445 (2003).
3. K. Ito, G. Caramori, S. Lim, T. Oates, K. F. Chung, P. J. Barnes, and I. M. Adcock, "Expression and activity of histone deacetylases in human asthmatic airways," *Am. J. Respir. Crit. Care Med.* **166**, 392–396 (2002).
4. B. W. Pogue, H. B. Kaufman, A. Zelenchuk, W. Harper, G. C. Burke, E. E. Burke, and D. M. Harper, "Analysis of acetic acid-induced whitening of high-grade squamous intraepithelial lesions," *J. Biomed. Opt.* **6**, 397–403 (2001).
5. C. Balas, "A novel optical imaging method for the early detection, quantitative grading, and mapping of cancerous and precancerous lesions of cervix," *IEEE Trans. Biomed. Eng.* **48**, 96–104 (2001).
6. T. T. Wu, J. Y. Qu, T. H. Cheung, S. F. Yim, and Y. F. Wong, "Study of dynamic process of acetic acid induced-whitening in epithelial tissues at cellular level," *Opt. Express* **13**, 4963–4973 (2005).
7. L. T. Perelman, V. Backman, M. Wallace, G. Zonios, R. Manoharan, A. Nusrat, S. Shields, M. Seiler, C. Lima, T. Hamano, I. Itzkan, J. Van Dam, J. M. Crawford, and M. S. Feld, "Observation of periodic fine structure in reflectance from biological tissue: a new technique for measuring nuclear size distribution," *Phys. Rev. Lett.* **80**, 627–630 (1998).
8. V. Backman, R. Gurjar, K. Badizadegan, R. Dasari, I. Itzkan, L. T. Perelman, and M. S. Feld, "Polarized light scattering spectroscopy for quantitative measurement of epithelial cellular structures in situ," *IEEE J. Sel. Top. Quantum Electron.* **5**, 1019–1026 (1999).
9. A. Wax, C. Yang, V. Backman, K. Badizadegan, C. W. Boone, R. R. Dasari, and M. S. Feld, "Cellular organization and substructure measured using angle-resolved low-coherence interferometry," *Biophys. J.* **82**, 2256–2264 (2002).
10. K. Sokolov, R. Drezek, K. Gossage, and R. Richards-Kortum, "Reflectance spectroscopy with polarized light: is it sensitive to cellular and nuclear morphology?" *Opt. Express* **5**, 302–317 (1999).
11. H. Fang, M. Ollero, E. Vitkin, L. M. Kimerer, P. B. Cipolloni, M. M. Zaman, S. D. Freedman, I. J. Bigio, I. Itzkan, E. B. Hanlon, and L. T. Perelman, "Noninvasive sizing of subcellular organelles with light scattering spectroscopy," *IEEE J. Sel. Top. Quantum Electron.* **9**, 267–276 (2003).
12. J. R. Mourant, J. P. Freyer, A. H. Hielscher, A. A. Eick, D. Shen, and T. M. Johnson, "Mechanisms of light scattering from biological cells relevant to noninvasive optical tissue diagnostics," *Appl. Opt.* **37**, 3586–3593 (1998).
13. R. Drezek, A. Dunn, and R. Richards-Kortum, "Light scattering from cells: finite-difference time-domain simulations and goniometric measurements," *Appl. Opt.* **38**, 3651–3663 (1999).
14. J. D. Wilson, C. E. Bigelow, D. J. Calkins, and T. H. Foster, "Light scattering from intact cells reports oxidative-stress-induced mitochondrial swelling," *Biophys. J.* **88**, 2929–2938 (2005).
15. J. R. Mourant, T. M. Johnson, S. Carpenter, A. Guerra, T. Aida, and J. P. Freyer, "Polarized angular dependent spectroscopy of epithelial cells and epithelial cell nuclei to determine the size scale of scattering structures," *J. Biomed. Opt.* **7**, 378–387 (2002).
16. H. C. van de Hulst, *Light Scattering by Small Particles* (Dover, 1981), 6 pp.
17. R. Drezek, A. Dunn, and R. Richards-Kortum, "A pulsed finite-difference time-domain (FDTD) method for calculating light scattering from cells over broad wavelength ranges," *Opt. Express* **6**, 147–157 (2000).